

## Synthesis of Mesoporous $\gamma$ -Al<sub>2</sub>O<sub>3</sub> Templated with Rosin-Based Quaternary Ammonium Salt by Ammonia Precipitation

PENG WANG, ZHENDONG ZHAO\*, LIANGWU BI and YUXIANG CHEN

Institute of Chemical Industry of Forest Products, CAF; National Engineering Lab. for Biomass Chemical Utilization, Key and Open Lab. on Forest Chemical Engineering, SFA, Nanjing 210042, P.R. China

\*Corresponding author: Fax: +86 25 85482455; Tel: +86 25 85482455; E-mail: zdzhao@189.cn

(Received: 7 July 2011;

Accepted: 6 March 2012)

AJC-11161

Mesoporous alumina were successfully synthesized by a facile method of ammonia precipitation with rosin-based quaternary ammonium salt. Their structures were characterized with X-ray diffraction, N<sub>2</sub> adsorption and desorption, transmission electron microscopy and thermal gravimetry-differential scanning calorimetry. The boehmite phase was achieved for precursors by ammonia precipitation, so that  $\gamma$ -Al<sub>2</sub>O<sub>3</sub> was easily prepared after the calcination at 550 °C for 4 h. These calcined materials possessed wormhole-like mesopores without long range packing order but with a fairly uniform pore size. The rosin-based quaternary ammonium salt dosage and aging temperature had great impact on the properties of the alumina. When the dosage of rosin-based quaternary ammonium salt was 1.6 g and the aging temperature was 90 °C, the maximum BET surface area (271 m<sup>2</sup> g<sup>-1</sup>), pore volume (0.59 cm<sup>3</sup> g<sup>-1</sup>) and pore size (6.39 nm) were obtained.

**Key Words:** Mesoporous alumina, Rosin-based quaternary ammonium salt,  $\gamma$ -Al<sub>2</sub>O<sub>3</sub>.

### INTRODUCTION

Since ordered mesoporous materials M41S were synthesized by Mobile corporation scientists<sup>1,2</sup>, a most important concept "templates" was introduced in the synthesis of mesoporous materials. Many kinds of surfactants were used as "templates" to produce variety of silica mesoporous materials, such as, SBA<sup>3-10</sup>, HMS<sup>11</sup>, MSU<sup>12</sup>, FDU<sup>13-18</sup>. New types of surfactants are still under pursuing for producing mesoporous materials with specific structures.

Alumina especially for  $\gamma$ -Al<sub>2</sub>O<sub>3</sub> was widely used as catalysts or supports in the petrochemical and chemical industry because of their big surface area, high activity and good hydrothermal stability. Compared with traditional  $\gamma$ -Al<sub>2</sub>O<sub>3</sub>, uniform mesoporous  $\gamma$ -Al<sub>2</sub>O<sub>3</sub> possess more attractive properties, such as a narrow pore size distribution, uniform pore channels and large pore diameter, which always have much impact on the catalytical performance. Therefore, great efforts have been paid for producing uniform mesoporous  $\gamma$ -Al<sub>2</sub>O<sub>3</sub> by using template agents (cationic, anionic, non-ionic surfactants or any other non-surfactant templates).

For the "non-ionic" route, González-Peña and coworkers<sup>19</sup> published the synthesis of uniform mesoporous alumina by using Tergitol 15-S-9 and Triton X-114 as a directing agent in the presence of dipropylamine. After calcination at 600 °C, the surface areas of all the samples were higher than 300 m<sup>2</sup> g<sup>-1</sup>.

However,  $\gamma$ -Al<sub>2</sub>O<sub>3</sub> was obtained only after calcination at 700 °C and the surface areas were 229-267 m<sup>2</sup> g<sup>-1</sup>. For the "anionic" route, Yada *et al.*<sup>20,21</sup> described the production of hexagonal mesostructure as-synthesized alumina by the homogeneous precipitation method using urea and sodium dodecylsulfate. Based upon this research, Sicard *et al.*<sup>22</sup> investigated the mechanism of the thermal decomposition of sodium dodecylsulfate. The pore volume and the surface area increased as the alkyl chain was removed below 473 and decreased as the sulfate head group was removed between 673 and 823 K. For the "cationic" route, Aguado and coworkers<sup>23</sup> reported the preparation of uniform mesoporous  $\gamma$ -Al<sub>2</sub>O<sub>3</sub> by sol-gel method using CTAB as a directing agent. The procedure was carried out in acidic medium with three steps (hydrolysis, condensation and calcination). The alumina showed surface areas larger than 300 m<sup>2</sup> g<sup>-1</sup>, pore diameters within the 4-15 nm range.

Some kinds of non-surfactant templates have also been introduced to synthesize mesoporous alumina. Hydrocarboxylic acid was used as a template by Liu *et al.*<sup>24</sup> with boehmite sol as the precursor. The obtained materials displayed high surface areas (380.9 m<sup>2</sup> g<sup>-1</sup>), uniform pore sizes and three-dimensional interconnected worm-like mesostructures. A series of mesoporous alumina was prepared using saccharide molecules including glucose, sucrose, starch and  $\beta$ -cyclodextrins as templates in the study of Xu *et al.*<sup>25,26</sup>. Sucrose templated alumina got the highest surface area (364 m<sup>2</sup> g<sup>-1</sup>).

with a pore size at 4.4 nm. The molecular size of the templates and the initial pH value of the system had a great effect on the physical properties of products.

In this work, rosin-based quaternary ammonium salt ( $C_{20}H_{29}N(CH_3)_3Cl$ , short for RQAS) was applied as a template agent to produce uniform mesoporous  $\gamma$ - $Al_2O_3$ . Unlike the traditional long chain surfactants, RQAS possesses a big group of a three-ring phenanthrene skeleton (**Scheme-I**) and as far as we know, it has not been used for preparing uniform mesoporous aluminas. Moreover, although the big surface area and pore sized were obtained in the works mentioned above, the expensive alkoxides or boehmite aluminum source and the complicated synthesis methods blocked the way toward industry application. Hence, a facile method of ammonia precipitation was employed with the assistant of this unique structural template, which offered us a chance of industry application. The rosin-based quaternary ammonium salt dosage and the aging temperature were adjusted to achieve the best properties.

## EXPERIMENTAL

Aluminium nitrate nonahydrate (AR) was purchased from Shanghai Zhenxin Reagent chemical Factory. Ammonia solution (AR 25 %) was purchased from Nanjing Chemical Reagent Co. Ltd. Rosin-based quaternary ammonium salt (technical grade, principal component: abietyltrimethyl ammonium chloride) was provided by Henan Titaning Chemical Technology Co. Ltd.

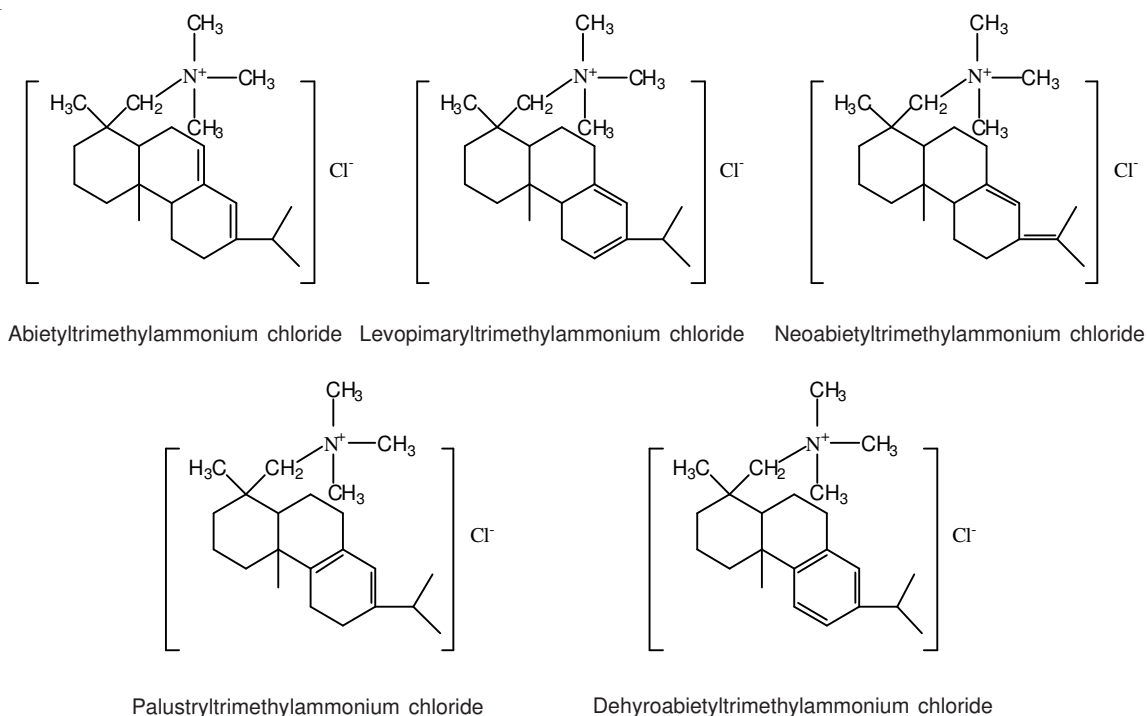
General procedure: In a typical experiment, 7.6 g  $Al(NO_3)_3 \cdot 9H_2O$  and rosin-based quaternary ammonium salt (0.8, 1.6, 3.3 and 4.1 g) were dissolved in 30 mL de-ionized water at 70 °C, respectively and 70 mL of ammonia solution (25 % water solution) was then added dropwise under stirring. The precipitated products were aged at 30, 50, 70 and 90 °C,

for 18 h and washed with hot water for several times to remove chloride ion. After drying at 90 °C, the template agents were removed by calcination at 550 °C for 4 h at a heating rate of 1 °C/min. The results were labeled as A-X-Y, X denoted the dosage of rosin-based quaternary ammonium salt and Y denoted the aging temperature.

**Detection method:** The crystalline phases of the alumina were recorded by a Bucker D8 Focus X-ray diffractometer with  $CuK_{\alpha}$  radiation ( $\lambda = 0.15418$  nm). The operating target voltage was 40 kV and the current was 40 mA. The sample was powdered and scanned for  $2\theta$  ranging from 0.5-5.0° for low-angle and 10-80° for high-angle. Porosity and surface area measurements were performed following the  $N_2$  adsorption on a Micromeritics ASAP2020 instrument made by Micromeritics Instrument Corporation. The special surface areas were calculated using the Brunauer-Emmett-Teller (BET) model. Average pore diameters were calculated using the Barrett-Joyner-Halenda (BJH) method from the desorption branch of isotherm. Transmission electron microscopy (TEM) images were obtained with a Jeol JEM-2100 instrument operating at an accelerating voltage 200 kV. The samples were ultrasonically dispersed in ethanol and then dropped onto the carbon-coated copper grids prior to the measurements. Thermogravimetry and differential scanning calorimetry (TG-DSC) was performed on a NETZSCH STA409PC thermogravimetric analyzer from 40-800 °C with a heating rate of 10 °C  $min^{-1}$  in air (20 mL  $min^{-1}$ ).

## RESULTS AND DISCUSSION

Low-angle XRD patterns of as-synthesized samples are depicted in Fig. 1(a and b). As seen in Fig. 1(a), the sample of A-0.8-90 shows no obvious diffraction peaks but a hump at  $2\theta = 1.12^\circ$ . The other three samples show a single sharp diffraction peak (A-1.6-90:  $2\theta = 0.76^\circ$ ; A-3.3-90:  $2\theta = 0.82^\circ$ ; A-4.1-90:  $2\theta = 0.78^\circ$ ) in the  $2\theta$  range from 0.5-5.0°, respectively.



**Scheme-I:** Structures of the main components in rosin-based quaternary ammonium salt

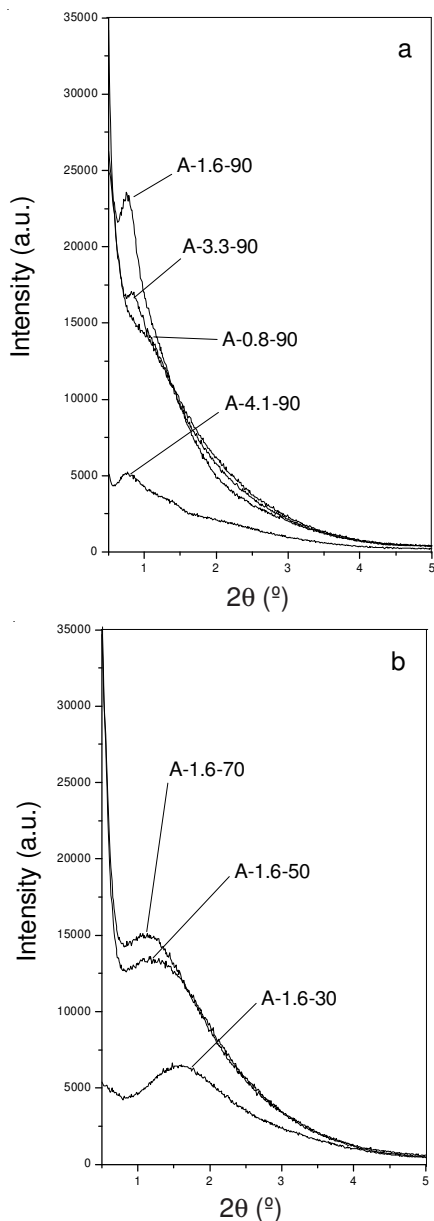


Fig. 1. Low-angle XRD patterns of as-synthesized samples. (a, rosin-based quaternary ammonium salt dosage: 0.8-4.1 g, aging temperature: 90 °C; b, rosin-based quaternary ammonium salt dosage: 1.6 g, aging temperature: 30-70 °C)

The intensity of the diffraction peaks enhances as the rosin-based quaternary ammonium salt dosage is increased, but decays abruptly with its farther increasing. As shown in Fig. 1(b), a single broad peak (A-1.6-30:  $2\theta = 1.62^\circ$ ; A-1.6-50:  $2\theta = 1.22^\circ$ ; A-1.6-70:  $2\theta = 1.13^\circ$ ) is observed in the  $2\theta$  range from  $0.5$ - $5.0^\circ$ , respectively. The diffraction peaks broaden and the intensity decreases as the aging temperature is decreased.

Low-angle XRD patterns of calcined alumina are presented in Fig. 2(a and b). All of the alumina exhibit an outstanding single diffraction peak in the  $2\theta$  range from  $0.5$ - $5.0^\circ$ , respectively. This low-angle XRD peak could be related to the mesoporous of alumina with a fairly uniform pore size but without a long range packing order<sup>27</sup>. The intensity of diffraction peaks for all of the samples increased because of the removal of the surfactants. As shown in Fig. 2(a), the diffraction peak of sample A-0.8-90 reveals at  $2\theta = 0.76^\circ$ , which is lower

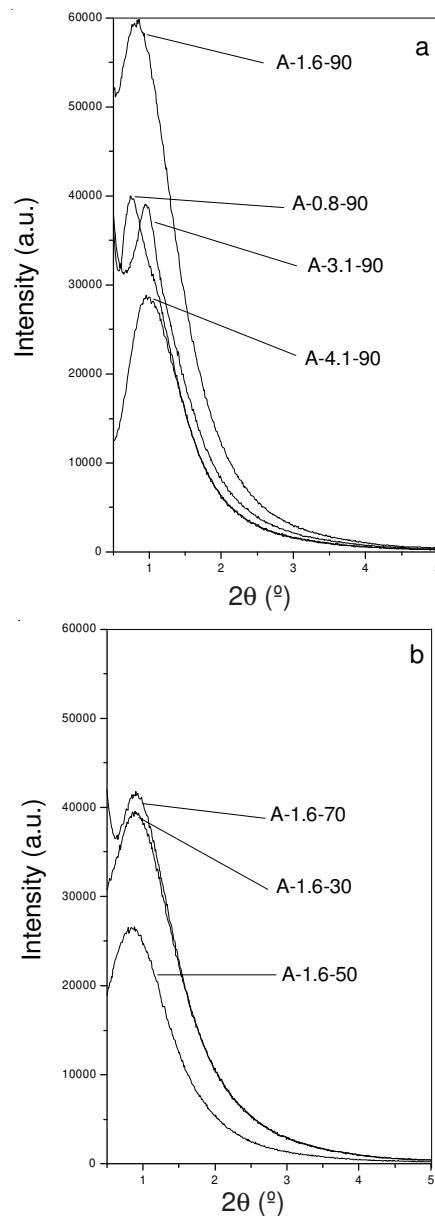


Fig. 2. Low-angle XRD patterns of calcined aluminas. (a, rosin-based quaternary ammonium salt dosage: 0.8-4.1 g, aging temperature: 90 °C; b, rosin-based quaternary ammonium salt dosage: 1.6 g, aging temperature: 30-70 °C)

than that of sample A-1.6-90 ( $2\theta = 0.86^\circ$ ), but lower than the other two samples (A-3.3-90:  $2\theta = 0.95^\circ$ ; A-4.0-90:  $2\theta = 0.98^\circ$ ). From Fig. 2(b) we can see, the diffraction peak intensity of the sample A-1.6-30 ( $2\theta = 0.91^\circ$ ) is stronger than the sample A-1.6-50 ( $2\theta = 0.85^\circ$ ) but weaker than the sample A-1.6-70 ( $2\theta = 0.90^\circ$ ), which means the trend shown in Fig. 1b can't maintain after calcinations.

High-angle XRD patterns of as-synthesized samples are illustrated in Fig. 3. All of the samples display diffraction peaks of the boehmite phase (JCPDS Card 21-1307). The diffraction peaks of the sample A-1.6-30 migrate to the low angle slightly with a diffusion appearance, which indicates that low ageing temperature can decrease the crystallinity. Fig. 4 shows the high-angle XRD patterns of calcined aluminas. All of the samples display the identical diffraction peaks which can be indexed to a  $\gamma$ -Al<sub>2</sub>O<sub>3</sub> phase with high crystallinity (JCPDS Card

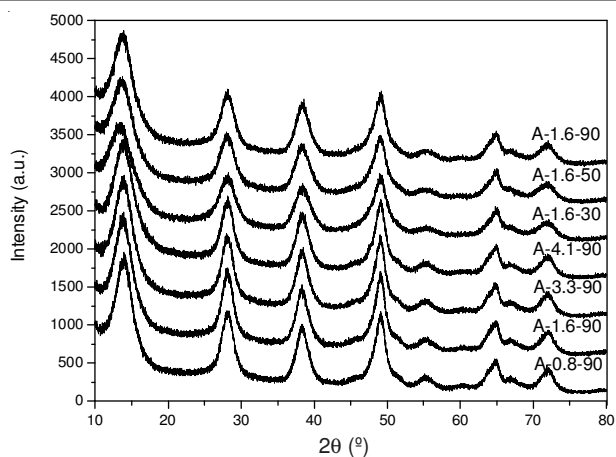


Fig. 3. High-angle XRD patterns of as-synthesized samples

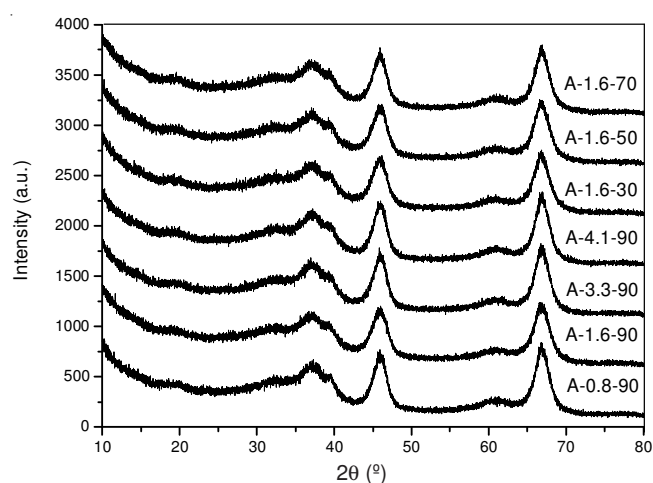


Fig. 4. High-angle XRD patterns of calcined aluminas

10-0425). No obvious dissimilarity can be observed in the calcined aluminas.

Transmission electron microscopy image of sample A-1.6-90 is given in Fig. 5(a-c). This material possesses worm-hole-like appearance without a long range packing order but with a fairly uniform pore size, which is in good agreement with the result of the absence of high order peaks in low angle X-ray diffraction pattern. Fig. 5(d) shows the electron diffraction pattern obtained from a selected area of Fig. 5(a), indicating the  $\gamma$ - $\text{Al}_2\text{O}_3$  phase is formed in this sample.

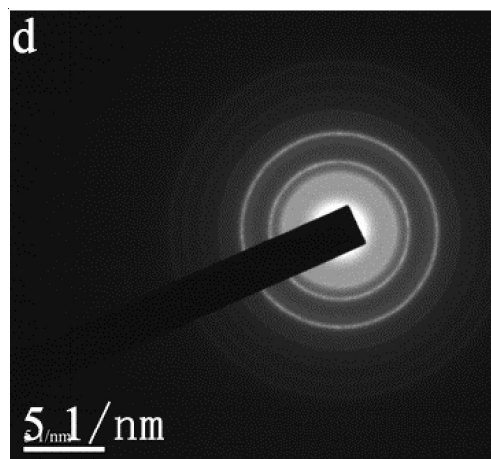
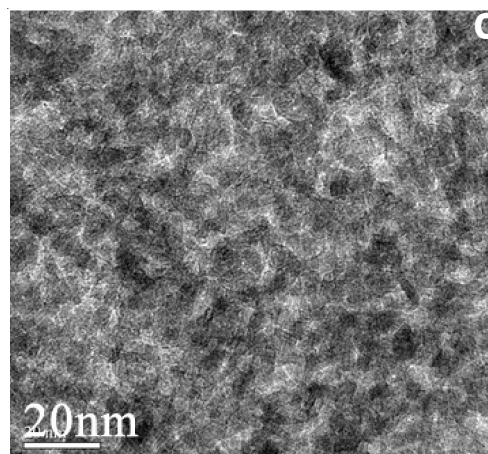
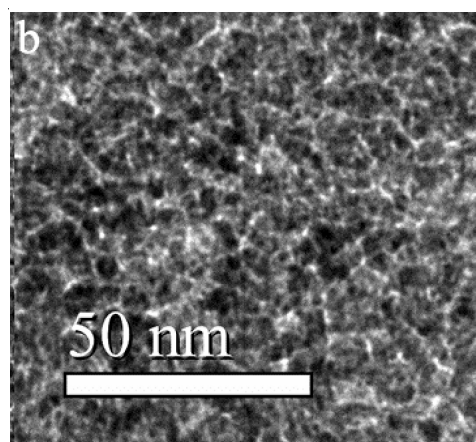
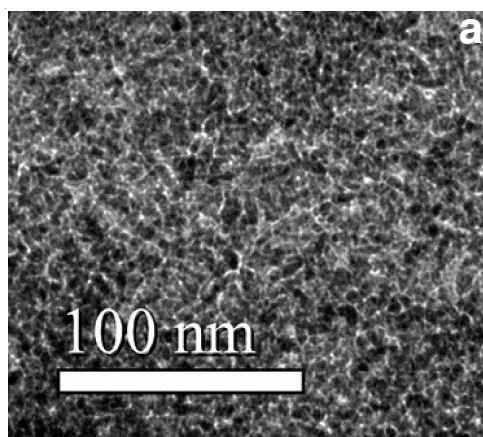


Fig. 5. TEM images (a, b and c) of calcined alumina A-1.6-90 and electron diffraction pattern (d) of a region of the same sample

$\text{N}_2$  adsorption-desorption isotherms are shown in Fig. 6. All the isotherms exhibit the classical type IV shape according to the IUPAC classification, indicating the presence of mesoporous structures in the calcined aluminas. BJH pore distributions of the calcined aluminas are presented in Fig. 7. All the samples show a narrow mesopore size distribution centered at about 7 nm. Calcined sample A-1.6-90 shows larger mesopores with narrower pore size distribution. Increasing or decreasing the rosin-based quaternary ammonium salt dosages results in lower pore sizes and broader pore size distribution. This trend can also be observed by decreasing aging temperature. Table-1 listed the textural properties of the calcined

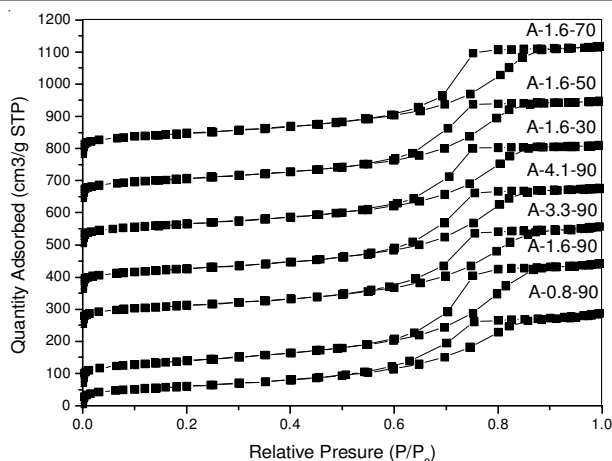
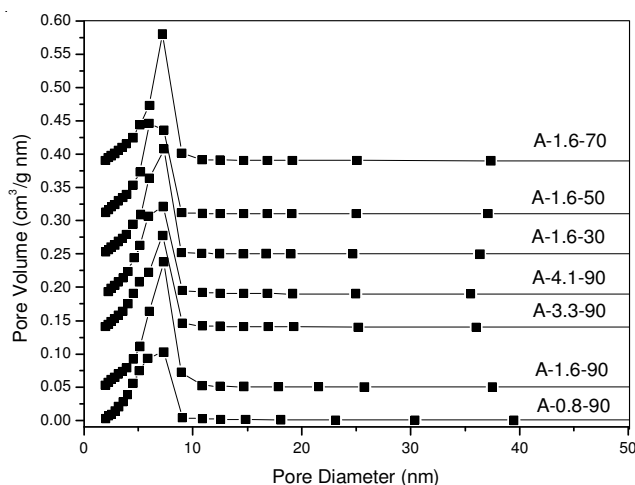
Fig. 6. N<sub>2</sub> adsorption-desorption isotherms of calcined alumina

Fig. 7. BJH pore distributions of calcined aluminas

Sample	S <sub>BET</sub> (m <sup>2</sup> g <sup>-1</sup> )	V (cm <sup>3</sup> g <sup>-1</sup> )	D (nm)
A-0.8-90	219	0.45	6.05
A-1.6-90	271	0.59	6.39
A-3.3-90	225	0.48	6.19
A-4.1-90	238	0.49	6.06
A-1.6-30	238	0.49	6.00
A-1.6-50	240	0.48	5.92
A-1.6-70	243	0.53	6.37

aluminas. The maximum BET surface area (271 m<sup>2</sup> g<sup>-1</sup>), pore volume (0.59 cm<sup>3</sup> g<sup>-1</sup>) and pore size (6.39 nm) is obtained for the calcined sample A-1.6-90. The increase or decrease of the rosin-based quaternary ammonium salt dosages can decrease the value of the textural properties and the decrease of the aging temperature can also decay the value of the textural properties.

TG-DSC curves of calcined alumina A-1.6-90 are plotted in Fig. 8. Three distinct steps of weight loss are discernible. The first weight loss below 150 °C can be related to the removal of physically absorbed water. The second weight loss between 150 and 418 °C with two exothermic peaks at 334 and 362 °C is due to the combustion of rosin-based quaternary ammonium salt surfactant and the decomposition of boehmite. The third weight loss above 418 °C is associated to the release of water resulting from the phase transformation to  $\gamma$ -Al<sub>2</sub>O<sub>3</sub><sup>28</sup>.

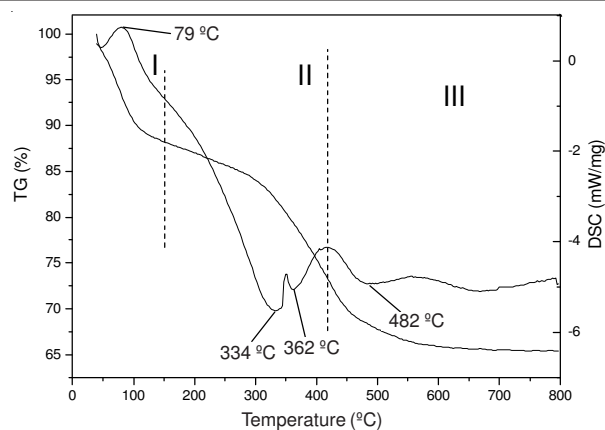


Fig. 8. TG-DSC curves of as-synthesized sample A-1.6-90

## Conclusion

A facile method of ammonia precipitation was used to synthesize mesoporous aluminas with the assistant of rosin-based quaternary ammonium salt. The precursors were boehmite phase and  $\gamma$ -Al<sub>2</sub>O<sub>3</sub> was prepared after the calcination at 550 °C for 4 h. These calcined materials possessed wormhole-like mesopores without long range packing order but with a fairly uniform pore size. The rosin-based quaternary ammonium salt dosage and aging temperature had great impact on the properties of the aluminas. When the dosage of rosin-based quaternary ammonium salt was 1.6 g and the aging temperature was 90 °C, the maximum BET surface area (271 m<sup>2</sup> g<sup>-1</sup>), pore volume (0.59 cm<sup>3</sup> g<sup>-1</sup>) and pore size (6.39 nm) were obtained. The increase or decrease of the rosin-based quaternary ammonium salt dosages could decrease the value of the textural properties and the decrease of the aging temperature could also decay the value of the textural properties.

## ACKNOWLEDGEMENTS

This work was supported by the Natural Science Foundation of China (grant No. 30972319) and the Joint Innovation of Industries, Universities and Research Institutes Foundation (grant No. BY2010112).

## REFERENCES

- C.T. Kresge, M.E. Leonowicz, W.J. Roth, J.C. Vartuli and J.S. Beck, *Nature*, **359**, 710 (1992).
- J.S. Beck, J.C. Vartuli, W.J. Roth, M.E. Leonowicz, C.T. Kresge, K.D. Schmitt, C.T.W. Chu, D.H. Olson, E.W. Sheppard, S.B. McCullen, J.B. Higgins and J.L.J. Schlenker, *Am. Chem. Soc.*, **114**, 10834 (1992).
- D. Zhao, J. Feng, Q. Huo, N. Melosh, G.H. Fredrickson, B.F. Chmelka and G.D. Stucky, *Science*, **279**, 548 (1998).
- Q. Huo, D.I. Margolese, U. Ciesla, D.G. Demuth, P. Feng, T.E. Gier, P. Sieger, A. Firouzi, B.F. Chmelka, F. Schüth and G.D. Stucky, *Chem. Mater.*, **6**, 1176 (1994).
- Q. Huo, D.I. Margolese and G.D. Stucky, *Chem. Mater.*, **8**, 1147 (1996).
- Q. Huo, D.I. Margolese, U. Ciesla, P. Feng, T.E. Gier, P. Sieger, R. Leon, P.M. Petroff, F. Schüth and G.D. Stucky, *Nature*, **368**, 317 (1994).
- Q. Huo, R. Leon, P.M. Petroff and G.D. Stucky, *Science*, **268**, 1324 (1995).
- D. Zhao, Q. Huo, J. Feng, B.F. Chmelka and G.D. Stucky, *J. Am. Chem. Soc.*, **120**, 6024 (1998).
- C. Yu, B. Tian, J. Fan, G.D. Stucky and D. Zhao, *J. Am. Chem. Soc.*, **124**, 4556 (2002).
- C.C. Pantazis and P.J. Pomonis, *Chem. Mater.*, **15**, 2299 (2003).
- P.T. Tanev and T.J. Pinnavaia, *Science*, **267**, 865 (1995).

12. S.A. Bagshaw, E. Prouzet and T.J. Pinnavaia, *Science*, **269**, 1242 (1995).
13. C.Z. Yu, Y.H. Yu and D.Y. Zhao, *Chem. Commun.*, 575 (2000).
14. X. Liu, B. Tian, C. Yu, F. Gao, S. Xie, B. Tu, R. Che, L.-M. Peng and D. Zhao, *Angew. Chem. Int. Ed.*, **41**, 3876 (2002).
15. J. Fan, C.Z. Yu, T. Gao, J. Lei, B.Z. Tian, L.M. Wang, Q. Luo, B. Tu, W.Z. Zhou and D.Y. Zhao, *Angew. Chem. Int. Ed.*, **42**, 3146 (2003).
16. Y. Meng, D. Gu, F.Q. Zhang, Y.F. Shi, L. Cheng, D. Feng, Z.X. Wu, Z.X. Chen, Y. Wan, A. Stein and D.Y. Zhao, *Chem. Mater.*, **18**, 4447 (2006).
17. Y. Huang, H.Q. Cai, T. Yu, F.Q. Zhang, F. Zhang, Y. Meng, D. Gu, Y. Wan, X.L. Sun, B. Tu and D.Y. Zhao, *Angew. Chem. Int. Ed.*, **46**, 1089 (2007).
18. Y.H. Deng, T. Yu, Y. Wan, Y.F. Shi, Y. Meng, D. Gu, L.J. Zhang, Y. Huang, C. Liu, X.J. Wu and D.Y. Zhao, *J. Am. Chem. Soc.*, **129**, 1690 (2007).
19. V. González-Peña, I. Díaz, C. Márquez-Alvarez, E. Sastre and J. Pérez-Pariente, *Micropor. Mesopor. Mater.*, **44-45**, 203 (2001).
20. M. Yada, H. Kitamura, M. Machida and T. Kijima, *Langmuir*, **13**, 5252 (1997).
21. M. Yada, H. Hiyoshi, K. Ohe, M. Machida and T. Kijima, *Inorg. Chem.*, **36**, 5565 (1997).
22. L. Sicard, P.L. Liewellyn, J. Patarin and F. Kolenda, *Micropor. Mesopor. Mater.*, **44-45**, 195 (2001).
23. J. Aguado, J.M. Escola, M.C. Castro and B. Paredes, *Micropor. Mesopor. Mater.*, **83**, 181 (2005).
24. Q. Liu, A. Wang, X. Wang and T. Zhang, *Micropor. Mesopor. Mater.*, **92**, 10 (2006).
25. B. Xu, T. Xiao, Z. Yan, X. Sun, J. Sloan, S.L. González-Cortés, F. Alshahrani and M.L.H. Green, *Micropor. Mesopor. Mater.*, **91**, 293 (2006).
26. B. Xu, J. Long, H. Tian, Y. Zhu and X. Sun, *Catal. Today*, **147S**, S46 (2009).
27. S.S. Kim, W.Z. Zhang and T.J. Pinnavaia, *Science*, **282**, 1302 (1998).
28. M.B. Yue, W.Q. Jiao, Y.M. Wang and M.Y. He, *Micropor. Mesopor. Mater.*, **132**, 226 (2010).